

Pamela T. Johnson · Laura M. Fayad ·
Elliot K. Fishman

Sixteen-slice CT with volumetric analysis of foot fractures

Received: 11 October 2005 / Accepted: 16 December 2005 / Published online: 28 March 2006
© Am Soc Emergency Radiol 2006

Abstract Computed tomography (CT) imaging of the foot demands excellent resolution for the delineation of complex fractures and joint alignment after trauma. The quality of current multislice volumetric acquisition results in exceptional multiplanar and 3-D reconstructions, precluding the requirement for an additional acquisition in a second plane. This pictorial essay depicts fractures of various bones of the foot, with reference to recent investigative studies demonstrating the value of CT in the evaluation of foot fractures.

Keywords Computed tomography · Computed tomography, multidetector row · Foot · Foot fracture · Three-dimensional rendering

Introduction

Musculoskeletal computed tomography (CT) of the trauma patient has been greatly enhanced by the implementation of multislice CT. Advantages of the new technology include speed of acquisition, improved resolution, and the ability to create multiplanar reconstructions from isotropic or near-isotropic data sets, rather than performing an additional acquisition in a second plane. Volumetric data sets, multiplanar reconstructions, and 3-D renderings have dramatically improved (Fig. 1) as a result of narrow collimation data acquisition and a decrease in motion

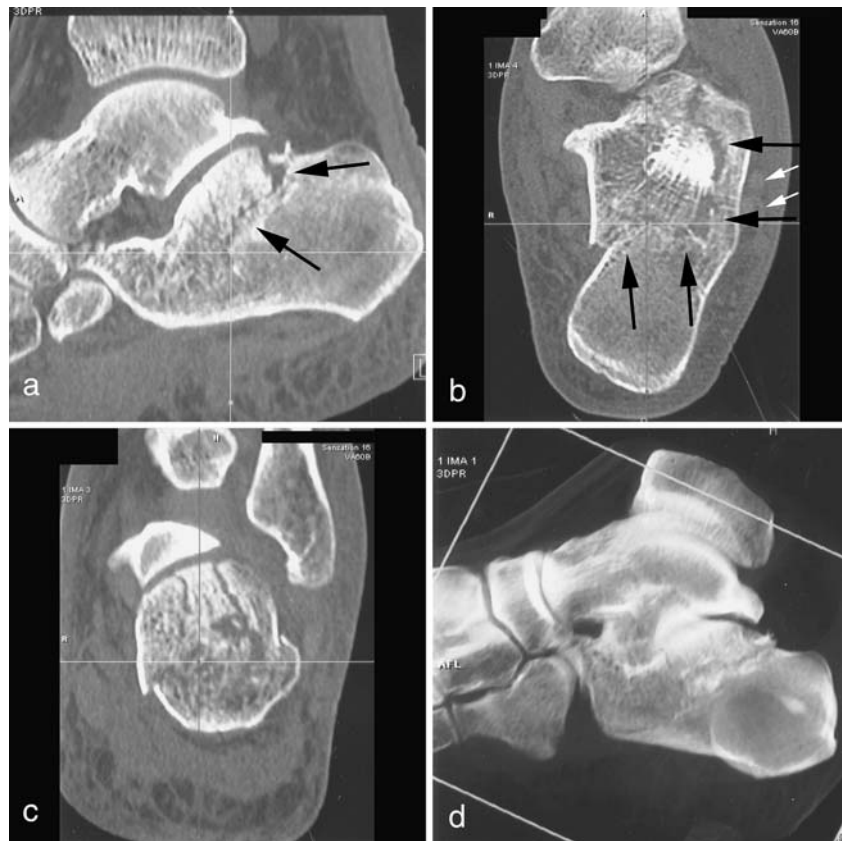
artifact. CT is essential for assessing complicated foot fractures, and data supports the use of CT for foot fracture



Fig. 1 A 15-year-old girl with a navicular fracture after a mountain biking accident. Anterior oblique 3-D CT image of the right foot shows the navicular fracture with widening of the fracture fragments and significant displacement and incongruity of the talonavicular joint. These findings necessitated surgery

P. T. Johnson · L. M. Fayad · E. K. Fishman (✉)
The Russell H. Morgan Department of
Radiology and Radiologic Sciences,
Johns Hopkins School of Medicine,
601 N. Caroline Street Room 3251,
Baltimore, MD 21287, USA
e-mail: efishman@jhmi.edu
Tel.: +1-410-9555173
Fax: +1-410-6140341

Fig. 2 A 48-year-old man with history of trauma to the foot and ankle. **a** Sagittal multiplanar reconstruction (MPR) CT image of the right foot and ankle shows a typical calcaneal fracture of “central depression” type, given the course of one of the major fracture lines (*black arrows*). **b** Axial oblique MPR CT image shows the two major fracture lines (*black arrows*). Note that the adjacent peroneal tendons (*white arrows*) are intact. **c** Coronal oblique MPR CT image shows clear extension of the fracture to the subtalar joint and minimal medial–lateral widening. **d** Sagittal volume-rendered, 3-D CT image for comparison demonstrates again the central depression type of fracture



detection in specific clinical scenarios [1, 2]. The purpose of this pictorial essay is to review some of the more common foot fractures and data that delineate the role of CT in their assessment.

Technique

Our protocol for 16 slice CT of the foot is as follows. The patient is positioned comfortably to limit movement. Using 120 kVp and 150–180 mA, we perform a single acquisition with detector row configuration of 16×0.75 mm. The

reconstruction slice thickness is .75 mm, with an interval of .5 mm. Data sets are reconstructed with both standard and bone algorithms. Two- and three-dimensional reconstructions are created with multiplanar reconstruction and interactive volume rendering (In Space, Siemens Medical Solutions, Malvern, PA), respectively.

Calcaneal fractures

In the foot, the calcaneus is the most frequently fractured bone [3, 4]. Causes of fracture of this bone include fall from



Fig. 3 A 35-year-old man who jumped from a building. **a** Coronal MPR CT image of the left foot and ankle shows a horizontal oblique fracture line in the calcaneus with slight medial–lateral widening and absence of involvement of the posterior facet. **b** Coronal volume-rendered 3-D CT image shows involvement of the middle facet with

a large sustentaculum fragment, suggesting a good prognosis for this fracture. **c** Sagittal volume-rendered 3-D CT image shows the two major fracture lines in the calcaneus, a typical “tongue-type” of calcaneal fracture

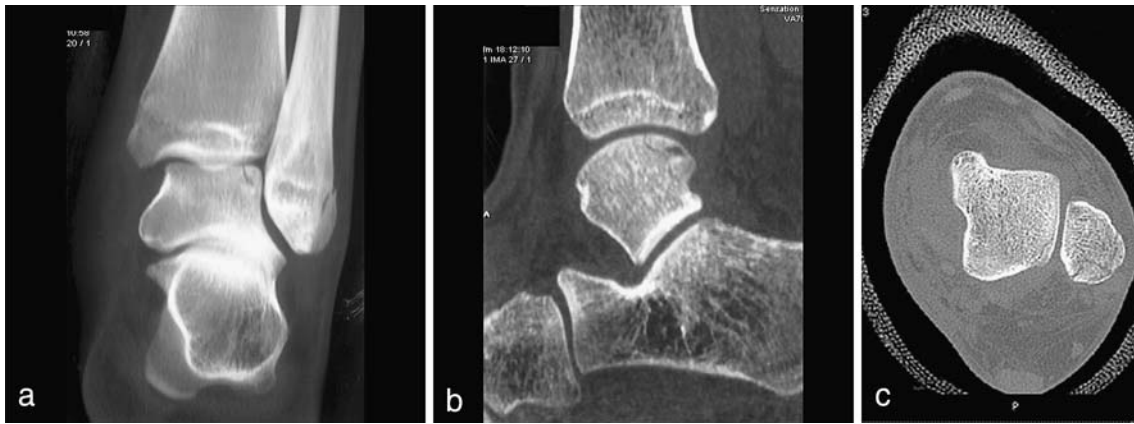


Fig. 4 A 16-year-old boy who sustained an inversion injury of the left ankle. **a** Coronal volume-rendered 3-D CT image of the left foot and ankle reveals fractures of the distal fibula and lateral talar dome. **b** Sagittal MPR CT image shows the posterolateral talar dome

fracture once again. **c** Axial CT image at the level of the tibiotalar joint shows the fractures. Note the overlying cast, which does not obscure the evaluation

a height, motorcycle and motor vehicle accidents [3–5]. Calcaneal fractures are classified as intra-articular and extra-articular. Intra-articular fractures (Figs. 2 and 3) are much more common and carry a worse prognosis than extra-articular fractures. Concomitant fractures may be identified in the contralateral calcaneus, ipsilateral lower extremity, and spine [3–5].

A study correlating fracture subtypes with postsurgical outcome revealed that central depression fractures (Fig. 2) were more likely to have an unsatisfactory result than tongue-type fractures (Fig. 3), but comminuted fractures had the worst outcome [6]. Using CT, Sanders [7] defined fracture subtypes based on number of fragments: undisplaced, 2-part, 3-part (split depression), and 4-part or highly comminuted. The latter had the worst postsurgical outcome.

Intra-articular fractures are often comminuted and may be displaced [8], requiring CT for accurate characterization. A recent study revealed that multiplanar four-slice CT is superior to conventional radiographs for elucidating the

extent of intra-articular calcaneal fractures and the location of the posterior calcaneal facet [1]. In a study comparing conventional radiographs, 2-D reformations, and 3-D renderings from helical CT data sets, 3-D CT was shown to be the superior display technique for multiple aspects of the evaluation [5]. These include identifying middle facet involvement in tongue-type fractures (Fig. 3), delineating the split when the posterior articular facet is divided into medial and lateral segments, correctly localizing the fracture line when a longitudinal tongue-type fracture line traverses the lateral calcaneus, characterizing joint depression fractures, and fully delineating intra-articular fracture involvement of the anterior process [5].

Several radiographic features of intra-articular fractures have been shown to correlate with the outcome. An unsatisfactory result is more likely in the setting of subtalar incongruity, grade 2 or 3 subtalar osteoarthritis, a decrease in fibulocalcaneal space (compared to the contralateral heel), and talonavicular joint osteoarthritis [6]. CT is

Fig. 5 A 31-year-old man who sustained a talar neck fracture after a motor vehicle accident. **a** Axial oblique MPR CT image of the right foot shows a talar neck fracture, with no talonavicular subluxation. **b** Coronal MPR CT image of the right foot shows the fracture extending to the subtalar joint, without evidence of tibiotalar subluxation or involvement

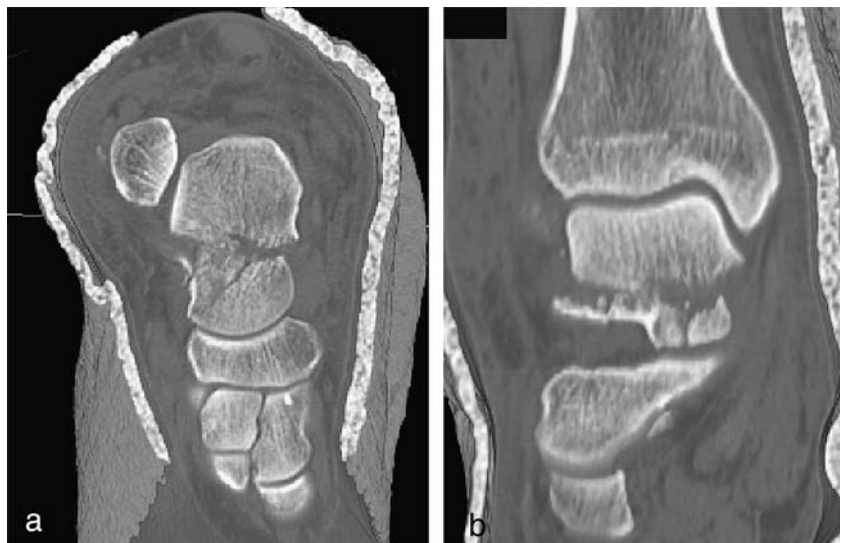
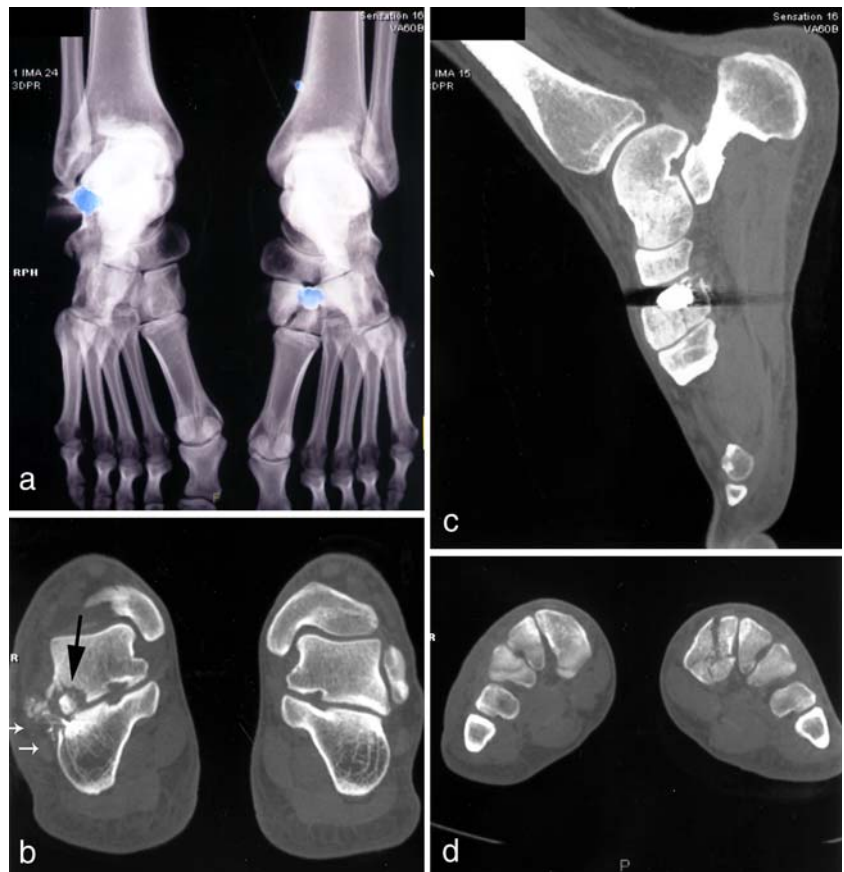


Fig. 6 A 20-year-old man who suffered gunshot wounds in both feet. **a** Axial oblique volume-rendered 3-D CT images of both feet reveal bilateral bullet fragments. The image was rendered to minimize metal artifact.

b Coronal MPR CT image of both feet shows a comminuted fracture of the lateral process of the talus, involvement of the posterior facet of the subtalar joint, and calcaneus with numerous fragments. Note the bullet fragment (*black arrow*) and the nearby peroneal tendons (*white arrows*). **c** Sagittal MPR CT image of the left foot reveals the bullet fragment with adjacent fracture of the medial cuneiform bone extending to the tarsal–metatarsal articulation.

d Coronal MPR CT image of the feet shows fracture of the cuneiform bone in cross-section. In this plane, it is difficult to evaluate extension of the fracture to the articular space



valuable after treatment to detect fracture malunion and secondary osteoarthritis [3].

Talar fractures

The talus is the second most common tarsal bone to fracture and is prone to dislocation after trauma due to a paucity of muscular attachments [3]. In Haapamaki's [1] study comparing multislice CT to conventional radiographs, radiographs had a lower sensitivity (78%) for talar fracture detection. Multislice CT was shown to be valuable in identifying isolated talar trochlea fractures (Fig. 4) and in detecting intra-articular fractures in the setting of subtalar or talonavicular dislocations [1].

Fractures of the talar neck (Fig. 5) are seen in the setting of high-energy trauma, such as motor vehicle or motorcycle accidents, fall from a height, pedestrian motor vehicle accident, and sports trauma [4, 8]. The mechanism includes a force from below with dorsiflexion of the foot [3, 4]. The Hawkins classification system is based on the presence and location (subtalar, tibiotalar, talonavicular) of subluxation and dislocation [9]. Because of the anatomy of the blood supply to the talus, dislocation often disrupts the vascularization of the bone [3, 8]. Osteonecrosis was identified radiographically in 49% of the patients in one series, with collapse of the talar dome occurring in 31%. Open fractures



Fig. 7 A 17-year-old girl who was involved in a motorcycle accident. Sagittal volume-rendered 3-D CT image of the right foot shows a fracture at the base of the third metatarsal (*arrow*)

Fig. 8 A 26-year-old man who injured his right foot. **a** Sagittal volume-rendered 3-D CT image of the right foot shows a fracture of the medial cuneiform with intra-articular extension. **b** Coronal volume-rendered 3-D CT image of the right foot shows the fracture on end. Metatarsal bones have been digitally removed from the reconstructed image



and those with comminution of the talar neck carried a higher risk of collapse [8].

CT is necessary for proper delineation of the extent of a talar fracture and is very useful for follow-up to determine joint alignment, to exclude any residual intra-articular bone fragments (Fig. 6), and to detect complications of nonunion and osteoarthritis [4, 8]. Secondary osteoarthritis of the ankle or subtalar joint can be debilitating, it and occurred in 54% of the patients in one series, particularly with open or comminuted fractures [8].

Metatarsal and other tarsal fractures

Metatarsal fractures (Fig. 7) are often readily detected on conventional radiographs of the foot, with the exception of avulsion fractures of the tip of the tuberosity at the base of the fifth metatarsal, which can require an anteroposterior ankle radiograph [10]. However, in the setting of a hyperflexion injury, a study by Preidler et al. [2] demonstrated the benefit of CT over conventional radiographs. Forty-nine patients with hyperflexion injuries to the foot

were evaluated with conventional radiographs, CT, and magnetic resonance (MR) imaging. A total of 53 metatarsal fractures and 41 tarsal fractures (Fig. 8) were identified on CT. MR detected only 41 of the 53 metatarsal fractures and 39 of the 41 tarsal fractures. The conventional radiographs revealed only 33 of the 53 metatarsal fractures and 20 of the 41 tarsal fractures. The most commonly fractured metatarsal bone was the second, and the cuboid was the most frequently fractured tarsal bone. This study also revealed that joint malalignment identified on CT and MR was missed on 50% of the weight-bearing radiographs [2]. The classic Lisfranc fracture dislocations involve various combinations of lateral displacement of the lateral four metatarsals and medial or lateral displacement of the first metatarsal in combination with fractures of the base of the first and/or second metatarsal [3, 4]. Associated fractures may be detected in the cuboid, cuneiform, and navicular [3, 4]. Multiplanar, multislice CT (Fig. 9) has been shown to be superior to conventional radiographs for delineating the fractures and malaligned joints in Lisfranc fracture-dislocations [1].



Fig. 9 A 48-year-old man with history of diabetes mellitus and neuropathic arthropathy. **a** Axial oblique MPR CT image of the left foot shows a divergent Lisfranc fracture dislocation (*thin arrow*). Fragmentation of the midfoot is present (*thick arrow*). **b** Sagittal oblique MPR CT image of the left foot shows an associated fracture

of the lateral cuneiform bone (*arrow*). **c** Sagittal oblique MPR CT image of the left foot again shows midfoot fragmentation and disorganization with dislocation of the navicular bone (*large arrow*). A second metatarsal base fracture is identified by the *small arrow*

Conclusion

CT is well-established as the imaging modality of choice for characterization of complex foot fractures. In addition, studies have elucidated the importance of CT for fracture detection after hyperextension injuries and severe trauma [1, 2], as well as the value of 3-D renderings for evaluation of complicated calcaneal fractures [5]. It is important to recognize that multiple fractures of different parts of the foot or ankle often coexist in the setting of severe trauma [1]. Multiplanar and 3-D rendered multislice CT serve as the optimal imaging modality in this setting to elucidate the extent of fracture and dislocation in the foot and to readily communicate this information to orthopedic surgeons for treatment planning.

References

1. Haapamaki VV, Kiuru MJ, Koskinen SK (2004) Ankle and foot injuries: analysis of MDCT findings. *Am J Roentgenol* 183:615–622
2. Preidler KW, Peicha G, Lajtai G et al (1999) Conventional radiography, CT and MR imaging in patients with hyperflexion injuries of the foot: diagnostic accuracy in the detection of bony and ligamentous changes. *Am J Roentgenol* 173:1673–1677
3. Resnick D, Goergen TG, Niwayama G (1989) Physical trauma. In: Resnick D (ed) *Bone and joint imaging*. WB Saunders, Philadelphia, PA, pp 859–863
4. Berquist TH (2000) Fractures/dislocations. In: Berquist TH (ed) *Radiology of the foot and ankle*, 2nd edition. Lippincott, Williams and Wilkins, Philadelphia, PA, pp 218–261
5. Prasarthitha T, Sethavanitch C (2004) Three-dimensional and two-dimensional computerized tomographic demonstration of calcaneus fractures. *Foot Ankle Int* 25:262–273
6. Paley D, Hall H (1993) Intra-articular fractures of the calcaneus. A critical analysis of results and prognostic factors. *J Bone Joint Surg Am* 75:342–354
7. Sanders R, Fortin P, DiPasquale T, Walling A (1993) Operative treatment in 120 displaced intra-articular calcaneal fractures. Results using a prognostic computed tomography scan classification. *Clin Orthop Relat Res* 290:87–95
8. Vallier HA, Nork SE, Barei DP, Benirschke SK, Sangeorzan BJ (2004) Talar neck fractures: results and outcomes. *J Bone Joint Surg Am* 86A:1616–1624
9. Hawkins LG (1970) Fractures of the neck of the talus. *J Bone Joint Surg Am* 52:991–1002
10. Pao DG, Keats TE, Dussault RG (2000) Avulsion fracture of the base of the fifth metatarsal not seen on conventional radiography of the foot: the need for an additional projection. *Am J Roentgenol* 175:549–552